2025 IEEE/SICE International Symposium on System Integration (SII)
January 21-24, 2025, Munich, Germany

Application of Passive Dynamic Walking Model to Gait Trajectory Estimation Using Inertial Measurement Units and LiDAR*

Haruki Kasai, Kiyoshi Irie and Kimitoshi Yamazaki, *Member, IEEE*

***Abstract*— This paper presents a method for accurately estimating gait trajectory. We have developed an approach that leverages observations from two inertial motion units (IMUs) attached to both insteps and light detection and ranging (LiDAR) mounted on the back. A key advantage of this method is that it does not require observing the person from a fixed point. However, there is potential to further improve the accuracy of the estimated gait trajectory, particularly because the geometry of the gait has been somewhat distorted. In this study, we introduce a passive dynamic walking (PDW) model to preserve gait geometry and detail the formulation for integrating it into the existing method. Additionally, we present a method to address trajectory discontinuities using the PDW model. The effectiveness of the method is explained based on the experimental results using real data.**

I. Introduction

During human walking, the right and left soles alternately make contact with the ground, and the body's center of gravity shifts as we push off from the ground. By understanding these foot movements, we can expect to develop various applications. These applications may include estimating the walking environment, understanding behavioral intentions, and even recording an individual's behavioral history.

The purpose of this study is to establish a method for accurately estimating gait trajectory. As a previous study toward this goal, the authors attached inertial measurement units (IMUs) to the insteps of both feet, as depicted in the lower right part of Fig. 1, and proposed a method for estimating foot trajectories from the data obtained [1]. Subsequently, we introduced a method involving a LiDAR mounted on a person's back, as shown in Fig. 1, where LiDAR-based odometry was calculated from the LiDAR's point cloud data, and the gait trajectory was refined using LiDAR-based odometry. One of the key advantages of this method is that it does not require observing a person from a fixed point, thereby eliminating restrictions on the moving environment or range of movement. However, there is still potential to enhance the accuracy of the estimated trajectory. Specifically, although global gait trajectories were corrected through optimization, the gait geometry became distorted. In this study, we propose incorporating a passive dynamic walking (PDW) model to preserve gait geometry and present its formulation along with validation results. The contributions of this paper are as follows:

- We propose the integration of a PDW model into the existing method and have developed a specific procedure for its incorporation and model selection.

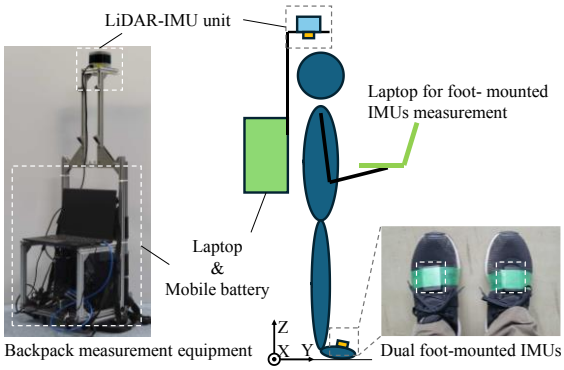

Fig.1. Overview of walking measurement equipment

- We explored a method to address trajectory discontinuities using the PDW model and validated its effectiveness with real-world data.

The structure of this paper is as follows. The next section reviews related work. Section III provides a brief overview of the previous methods, the challenges they encountered, and our approach in this study. Section IV details the method for incorporating the PDW model and offers a comprehensive explanation of the gait trajectory estimation process. Section V presents the validation results using real data, and Section VI concludes the study with a summary.

II. Related Work

Position estimation using inertial measurements typically faces the challenge of rapidly accumulating errors owing to the double integration of angular velocity and acceleration over time. In gait estimation, the zero velocity update (ZUPT) method is widely recognized for mitigating this issue [2]. A well-established approach employing ZUPT involves fusing sequential state predictions—derived from integrating angular velocity and acceleration—with zero-velocity observations obtained through ZUPT, using an extended Kalman filter (EKF) [3,4]. This method has been reported to achieve high accuracy in estimating movement. In approaches where IMUs are attached to both feet [5,6] and in those where additional sensors are collocated with the IMUs [7,8], the EKF is employed to integrate constraints based on the positional relationship between the left and right feet. While these methods have improved the accuracy of movement estimation, they do not address the shape of the trajectory.

The work presented in [9] uses optimization-based gait trajectory estimation, incorporating visual–inertial data

*This research is partly supported by JST [Moonshot R&D][Grant Number JPMJMS2034]. H. Kasai is with the Graduate School of Science and Technology, Shinshu University. K. Irie is with Future Robotics Technology Center, Chiba Institute of Technology, Tsudanuma 2-17-1, Narashino, Chiba, Japan. K. Yamazaki is with Faculty of Engineering, Shinshu University, Wakasato 4-17-1, Nagano, Nagano, Japan (corresponding author to provide phone: +81-26-269-5155; e-mail: kyamazaki@shinshu-u.ac.jp).

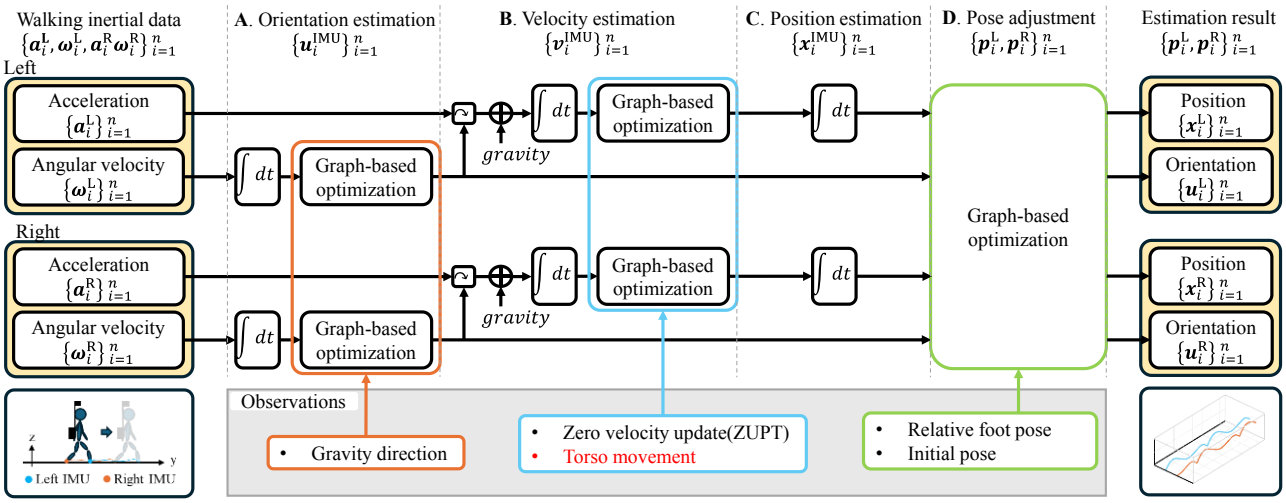

Fig. 2. Overview of gait trajectory estimation

obtained from Google Glass. The correspondence between the head and feet is taken into account during the period when both feet are in contact with the ground. During the period when both feet are on the ground, constraints are applied to ensure that the projection of the head onto the ground plane falls between successive footsteps. However, this method does not account for the correspondence during the swing phase, when the feet are in the air while walking. Other approaches involve using additional sensors, such as 17 IMUs distributed across the body, a LiDAR mounted at the center of gravity on the back [10], or a camera mounted on the head [11]. These methods allow for robust whole-body pose estimation even as walking distance increases, owing to the greater number of sensors. Conversely, when focusing solely on gait trajectory estimation, it is possible to reduce the number of sensors used.

Therefore, this study adopts a strategy of using additional sensors to estimate gait trajectory more accurately, with a particular focus on preserving the geometry of the gait trajectory in the results. We also explore constraint methods for the swing phase using a minimal sensor set, including IMUs and LiDAR-based odometry and apply these methods to optimization-based approaches.

III. Previous Method and Issues

A. Overview

To solve the problem of cumulative error associated with integration, Irie [12] succeeded in reducing the estimation error by using graph-based optimization. In gait trajectory estimation [1], this method is extended to integrate all five observations listed below through optimization.

- Sequential state changes by integrating acceleration and angular velocity from the IMUs,
- Observation of tilt relative to the direction of gravity to correct cumulative orientation errors,
- Observation of zero velocity points to correct cumulative velocity errors,
- Pseudo-observation based on the positional relationship between the left and right IMUs,
- Pseudo-observation providing the initial position for the estimation.

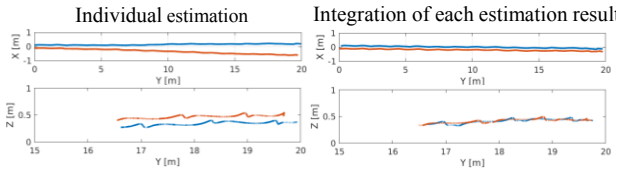

Fig. 3. Gait geometry after the individual estimation and integration of each result from 20 m of straight walking data. The top row shows the trajectory from the horizontal plane, while the bottom row shows the trajectory from the sagittal plane (for the last 5-s).

Additionally, the enhanced method presented in [13] incorporated a new observation of torso movement using rear-mounted LiDAR, as illustrated in Fig. 1. The relationship between the relative velocities of the torso and the insteps was integrated as constraints in the velocity optimization, as indicated by the red text in Fig. 2.

Fig. 2 illustrates the overall framework for gait trajectory estimation used in this study. The inputs consist of motion data from each foot obtained via IMUs and torso movement data (LiDAR-based odometry) derived from the LiDAR mounted on the back. The gait trajectory estimation process involves three main steps. First, individual estimations are performed for each IMU's data, correcting accumulated errors relative to the horizontal plane, excluding the nose azimuth (Fig. 2, A). Next, using ZUPT, accumulated errors in the velocity component are corrected by applying constraints that ensure foot velocity at rest is zero (Fig. 2, B). Finally, the estimation results are integrated, and the positioning of the left and right feet is adjusted (Fig. 2, D).

B. Issues Remaining in Previous Methods

The pseudo-observation of both feet positions, as introduced in [1], allows for correction of the positional relationship from a global perspective. However, an issue arises where the geometry of the gait trajectory is distorted owing to optimization. Fig. 3 shows the results estimated by the method in [13], where a person walked straight for 20 m. The integrated data from both feet shows that the original gait trajectory has become excessively smooth. There is a trade-off: while adjusting constraint weights can prevent such a result, it also reduces the effectiveness of foot positioning correction.

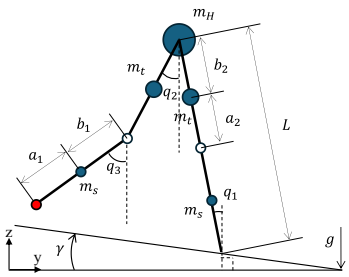

Parameters

m_H	Hip mass
m_s	Lower leg mass
m_t	Upper leg mass
l_s	Lower leg length
l_t	Upper leg length
$L = l_s + l_t$	
$l_s = a_1 + b_1$	
$l_t = a_2 + b_2$	
γ	Slope
q_1, q_2, q_3	Angle
$\dot{q}_1, \dot{q}_2, \dot{q}_3$	Angular velocity

a_1	0.375
b_1	0.125
a_2	0.175
b_2	0.325

m_H	0.5
m_t	0.5
m_s	0.05
γ	0.0504

q_1	0.1877
q_2	-0.2884
q_3	-0.2884

$\dot{q}_1$	-1.1014
$\dot{q}_2$	-0.0399
$\dot{q}_3$	-0.0399

Fig. 4. The kneed walker and physical parameters

While we presented an additional approach in [13] using body movement estimated from LiDAR data obtained from a measurement device similar to the one shown in Fig.1, this is insufficient for capturing detailed local geometry, such as gait trajectories. To address this issue, a more detailed formulation of the relative velocity relationship between the torso and feet during walking is necessary. This requires additional sensors because there is insufficient information about the thighs and lower legs to apply kinematic analysis. Alternatively, using a regression approach is another choice, but it requires prior data collection, which involves considerable effort.

C. Our Approach

Based on the abovementioned discussion, we propose a novel constraint designed to preserve the gait geometry during the individual estimation of foot trajectories. To maintain accurate gait geometry, it is essential to consider the relationship between the body and feet at each moment. Thus, we employ the PDW scheme, which generates a natural gait through the interaction between the dynamics of a machine and a slope [14, 15]. Research has shown that PDWs and human walking share similarities in energy efficiency [16]. We propose that the foot trajectory of a PDW resembles human gait and use this similarity to correct cumulative errors in the IMU data.

IV. Gait Trajectory Estimation Method

A. Assumptions for Adding Constraints on PDW

To correct the cumulative error in the foot trajectory $\{\boldsymbol{x}_i^{\mathrm{L}}\}_{i=1}^{n}$ and $\{\boldsymbol{x}_i^{\mathrm{R}}\}_{i=1}^{n}$ of the human gait, we improve the part of the velocity constraint in the previous method [8] regarding the observation of torso movement. Where n is the amount of data measured at the step time Δt. This observation, obtained via LiDAR-based odometry, is used as a velocity constraint rather than a position constraint. The reason is as follows. The error model addressed by graph-based optimization is a normal distribution with a mean of zero and the velocity errors accumulated from integrating acceleration in the IMU data are effectively reset at each walking cycle owing to the ZUPT effect. Therefore, the error can be considered normally distributed because it remains close to zero during the walking period. However, the cumulative error at the position stage—where velocity is further integrated—is treated as a bias error because it diverges indefinitely over time. In other words, this type of error is not manageable by the current method.

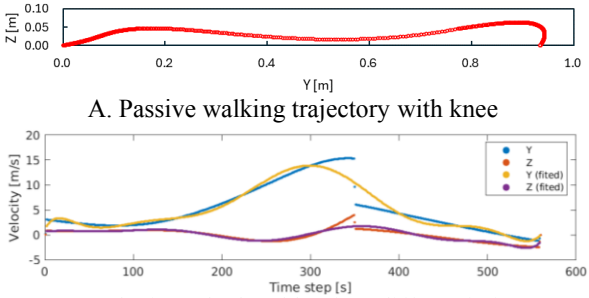

A. Passive walking trajectory with knee

B. Velocity calculated by time differentiation

Fig.5. Trajectory and velocity of the point foot in passive dynamic walking with a knee

For the PDW model, we use the point-foot model [17], which includes a knee joint similar to that of humans but features a simplified foot represented as a point (Fig. 4). The physical parameters are directly derived from the values presented in [17]. Given each joint angle q_1, q_2, q_3, the two-dimensional trajectory of the point foot in the sagittal plane is calculated using kinematics. This trajectory is then rotated and scaled in post-processing to align with the actual walk in the horizontal plane. The resulting trajectory is used to establish the correspondence between the torso and the feet in the velocity constraints based on torso movement observations.

B. Estimation of Foot Velocity for PDW

The following steps outline the process for converting the first step foot trajectory $\{\boldsymbol{x}_i^{\mathrm{PDW}}\}_{i=1}^{k}$ obtained from PDW simulation into velocity $\{\boldsymbol{v}_i^{\mathrm{PDW}}\}_{i=1}^{k}$ for applying constraints.

Rotation and scaling: Because the PDW involves motion on a slope, the slope component is removed by applying the rotation matrix R(γ), where γ is the slope angle, to obtain a walking trajectory on flat ground. Additionally, the stride length is adjusted using observations of torso movement. A single gait cycle T_m is defined as the period from when the foot leaves the ground to when it touches the ground again. The stride length is then calculated based on the principle that the amount of body movement corresponds to the amount of foot movement. The following equation is used:

$$\boldsymbol{x}_i^{\mathrm{PDW}'} = \frac{s_m^{\mathrm{Torso}}}{s^{\mathrm{PDW}}} \mathrm{R}(\gamma) \boldsymbol{x}_i^{\mathrm{PDW}}. \tag{1}$$

This means that s_m^{Torso} is the amount of torso movement during the m-th step of a gait cycle, and it is used to adjust the stride width s^{PDW} in the PDW model.

Velocity calculation by temporal differentiation: Instep velocity is determined by taking the temporal derivative of $\{\boldsymbol{x}_i^{\mathrm{PDW}'}\}_{i=1}^{k}$. The time increments used for this calculation differ from those employed in the PDW simulation owing to the abovementioned scaling. The following equation is used to calculate the velocity $\{\boldsymbol{v}_i^{\mathrm{PDW}'}\}_{i=1}^{k}$:

$$\boldsymbol{v}_i^{\mathrm{PDW}'} = \frac{\boldsymbol{x}_{i+1}^{\mathrm{PDW}'} - \boldsymbol{x}_i^{\mathrm{PDW}'}}{\Delta t_m}. \tag{2}$$

where Δt_m is the time increments, and k is the amount of data collected during T_m.

Velocity polynomial curve fitting: It is important to note when using temporal differentiation that, although the

trajectory of the PDW model appears smooth, there are points where the velocity changes abruptly, as illustrated in Fig. 5-B. This abrupt change occurs during the knee strike while the leg is swinging, when the PDW model transitions from the double pendulum equation of motion to that of a single pendulum at this specific moment. To address such sudden changes, we introduce a method that fits a polynomial approximation to smooth $\{\boldsymbol{v}_i^{\mathrm{PDW}'}\}_{i=1}^{k}$ and applies the recalculated velocity $\{\boldsymbol{v}_i^{\mathrm{PDW}}\}_{i=1}^{k}$ from this approximation to the constraint. The approximation is performed using a 10th-order polynomial for each axis for each step.

C. Individual Estimation

Among the time-series data, the moments when the velocity values of the IMUs reach zero are detected separately for the left and right sides in advance. Specifically, the acceleration norm in the series of movements from the start to the end of walking is filtered by high-pass and low-pass filters, and stationarity is determined by applying a threshold.

Next, the time-series orientation $\boldsymbol{U} = \{\boldsymbol{u}_i\}_{i=1}^{n}$ is estimated individually for each IMU data set. As a preliminary step for this optimization, an initial estimation is performed using the following integral, based on the observed angular velocities:

$$\boldsymbol{u}_{i+1} = \boldsymbol{u}_i * (\boldsymbol{\omega}_i \Delta t), \tag{3}$$

where $\boldsymbol{\omega}_i$ is a 3-dimensional angular velocity vector, and $\boldsymbol{u}_i$ is also a 3-dimensional vector [18] at time i. When treated as a rotation matrix, it is denoted as $\mathrm{R}(\boldsymbol{u}_i)$. The asterisk (*) indicates the coupling of the rotations. Subsequently, these results are modified by comparing the observed acceleration at rest with the direction of gravity. This refinement involves solving the following optimization problem [1]:

$$\boldsymbol{U}^* = \min F^{(\mathrm{u})}(\boldsymbol{U}), \tag{4}$$

$$F^{(\mathrm{u})}(\boldsymbol{U}) \coloneqq \sum_{i=1}^{n-1} \boldsymbol{e}_i^{(\omega)\top} \boldsymbol{\Omega}_i^{(\omega)\top} \boldsymbol{e}_i^{(\omega)\top} + \sum_{i \in C} \boldsymbol{e}_i^{(\mathrm{g})\top} \boldsymbol{\Omega}_i^{(\mathrm{g})\top} \boldsymbol{e}_i^{(\mathrm{g})\top}, \tag{5}$$

$$\boldsymbol{e}_i^{(\omega)} \coloneqq (-\boldsymbol{\omega}_i \Delta t) * (-\boldsymbol{u}_i) * \boldsymbol{u}_{i+1}, \tag{6}$$

$$\boldsymbol{e}_i^{(\mathrm{g})} \coloneqq \begin{bmatrix} \phi_i \\ \psi_i \end{bmatrix} - \begin{bmatrix} \phi_i^{acc} \\ \psi_i^{acc} \end{bmatrix}, \tag{7}$$

where $\boldsymbol{e}_i^{(\omega)}$ is based on time-series angular velocity observations, and $\boldsymbol{e}_i^{(\mathrm{g})}$ is based on gravity acceleration observations. $\boldsymbol{\Omega}$ is the inverse variance–covariance matrix of the observation error. ϕ_i and ψ_i denote the roll and pitch angles of the orientation $\boldsymbol{u}_i$ in the inertial coordinate system, whereas ϕ_i^{acc} and ψ_i^{acc} are the corresponding angles estimated from acceleration observations. This problem is a nonlinear least-squares problem and can be addressed using the Gauss–Newton method.

Alternatively, the time-series velocity $\boldsymbol{V} = \{\boldsymbol{v}_i\}_{i=1}^{n}$ is estimated in two steps: first, through integration, and then by correcting cumulative errors. In the first step, the following equation is used to obtain the velocity estimates.

$$\boldsymbol{v}_{i+1} = \boldsymbol{v}_i + (\mathrm{R}(\boldsymbol{u}_i)\boldsymbol{a}_i - \boldsymbol{g})\Delta t, \tag{8}$$

where $\boldsymbol{a}_i$ is a 3-dimensional acceleration vector and $\boldsymbol{g}$ is the gravity acceleration vector. These results are then refined using the stationary points. To achieve this, the following optimization problem is solved:

$$\boldsymbol{V}^* = \min F^{(\mathrm{v})}(\boldsymbol{V}), \tag{9}$$

$$F^{(\mathrm{v})}(\boldsymbol{V}) \coloneqq \sum_{i=1}^{n-1} \boldsymbol{e}_i^{(\mathrm{a})\top} \boldsymbol{\Omega}_i^{(\mathrm{a})} \boldsymbol{e}_i^{(\mathrm{a})} + \sum_{i \in C} \boldsymbol{e}_i^{(\mathrm{s})\top} \boldsymbol{\Omega}_i^{(\mathrm{s})} \boldsymbol{e}_i^{(\mathrm{s})} + \sum_{i \in \bar{C}} \boldsymbol{e}_i^{(t)\top} \boldsymbol{\Omega}_i^{(t)} \boldsymbol{e}_i^{(\mathrm{t})}, \tag{10}$$

$$\boldsymbol{e}_i^{(\mathrm{a})} \coloneqq -(R(\boldsymbol{u}_i)\boldsymbol{a}_i - \boldsymbol{g})\Delta t - \boldsymbol{v}_i + \boldsymbol{v}_{i+1}, \tag{11}$$

$$\boldsymbol{e}_i^{(\mathrm{s})} \coloneqq \boldsymbol{v}_i, \tag{12}$$

$$\boldsymbol{e}_i^{(\mathrm{t})} \coloneqq \boldsymbol{v}_i - \boldsymbol{v}_i^{\mathrm{PDW}}. \tag{13}$$

where $\boldsymbol{e}_i^{(\mathrm{a})}$ is based on time-series acceleration observations, and $\boldsymbol{e}_i^{(\mathrm{s})}$ is based on the assumption that the velocity is zero when stationarity is detected. $\boldsymbol{e}_i^{(\mathrm{t})}$ is a new component introduced in the proposed method, representing the error between the PDW foot velocity and the IMU velocity. Because the PDW used in this study operates in a two-dimensional sagittal plane, $v_{x,i}^{\mathrm{PDW}}$ is set to zero, and only the y and z axes are constrained. This forms a nonlinear least-squares problem that can be efficiently solved using the Newton method because the Hessian matrix of the objective function can be computed easily.

Using the obtained results, the position series for each IMU can be estimated. Specifically, the estimated velocities are integrated using the following equation:

$$\boldsymbol{x}_{i+1} = \boldsymbol{x}_i + \boldsymbol{v}_i \Delta t. \tag{14}$$

Finaly, all the estimated orientation, velocity, and position of IMUs are individually obtained.

D. Integration of Each Estimation Result

The position $\boldsymbol{x}_i$ and orientation $\boldsymbol{u}_i$, obtained through individual estimation, are combined and referred to as the 6-DoF pose $\boldsymbol{p}_i$. Let $\boldsymbol{P} = \{\boldsymbol{p}_i^{\mathrm{L}}, \boldsymbol{p}_i^{\mathrm{R}}\}_{i=1}^{n}$ be the combined state vector of the two poses, and $\boldsymbol{d}_i^{\mathrm{LR}} \coloneqq \boldsymbol{p}_i^{\mathrm{L}} \ominus \boldsymbol{p}_i^{\mathrm{R}}$ be the left foot pose relative to the right foot, where $\ominus$ is the operator to obtain the relative positions.

To correct the left–right positional relationship, the following optimization problem is solved [1]:

$$\boldsymbol{P}^* = \min F^{(\mathrm{p})}(\boldsymbol{P}), \tag{16}$$

$$F^{(\mathrm{p})}(\boldsymbol{P}) \coloneqq \sum_{i=1}^{n-1} \boldsymbol{e}_i^{\mathrm{L}(\mathrm{p})\top} \boldsymbol{\Omega}_i^{\mathrm{L}(\mathrm{p})} \boldsymbol{e}_i^{\mathrm{L}(\mathrm{p})} + \sum_{i=1}^{n-1} \boldsymbol{e}_i^{\mathrm{R}(\mathrm{p})\top} \boldsymbol{\Omega}_i^{\mathrm{R}(\mathrm{p})} \boldsymbol{e}_i^{\mathrm{R}(\mathrm{p})} + \sum_{i=1}^{n} \boldsymbol{e}_i^{\mathrm{LR}\top} \boldsymbol{\Omega}_i^{\mathrm{LR}} \boldsymbol{e}_i^{\mathrm{LR}} + \boldsymbol{e}_0^{\mathrm{L}\top} \boldsymbol{\Omega}^{\mathrm{E}} \boldsymbol{e}_0^{\mathrm{L}} + \boldsymbol{e}_0^{\mathrm{R}\top} \boldsymbol{\Omega}^{\mathrm{E}} \boldsymbol{e}_0^{\mathrm{R}}, \tag{17}$$

$$\boldsymbol{e}_i^{(\mathrm{p})} \coloneqq \boldsymbol{p}_{i+1} \ominus \boldsymbol{p}_i \ominus \begin{bmatrix} \Delta \boldsymbol{x}_i \\ \Delta \boldsymbol{u}_i \end{bmatrix}, \tag{18}$$

$$\begin{bmatrix} \Delta \boldsymbol{x}_i \\ \Delta \boldsymbol{u}_i \end{bmatrix} \coloneqq \begin{bmatrix} \boldsymbol{x}_{i+1} \\ \boldsymbol{u}_{i+1} \end{bmatrix} \ominus \begin{bmatrix} \boldsymbol{x}_i \\ \boldsymbol{u}_i \end{bmatrix}, \tag{19}$$

$$\boldsymbol{e}_i^{\mathrm{LR}} \coloneqq \boldsymbol{d}_i^{\mathrm{LR}} \ominus \boldsymbol{d}_0^{\mathrm{LR}}, \tag{20}$$

where $\Delta \boldsymbol{x}_i$ and $\Delta \boldsymbol{u}_i$ are the individually estimated differences in position and orientation, respectively. $\boldsymbol{e}_i^{\mathrm{LR}}$ is based on the pseudo-observation of the positional relationship between the left and right feet, serving as a constraint to ensure the feet are not excessively apart. $\boldsymbol{e}_0^{\mathrm{L}}$ and $\boldsymbol{e}_0^{\mathrm{R}}$ are terms that account for errors in the initial pose of each foot.

Table. I. The names of the comparison methods, the observations used for estimation, and the terminal errors of the resulting estimation.

Method names	Observations to be used	Terminal error [m]
Without LIO	Gravity direction, ZUPT	1.06
LIO velocity ×2	Gravity direction, ZUPT, torso movement [13] ($\boldsymbol{e}^{(\mathrm{t})} = \boldsymbol{v}^{\mathrm{IMU}} - 2\boldsymbol{v}^{\mathrm{LIO}}$)	0.51
PDW normal	Gravity direction, ZUPT, torso movement ($\boldsymbol{e}^{(\mathrm{t})} = \boldsymbol{v}^{\mathrm{IMU}} - \boldsymbol{v}^{\mathrm{PDW}'}$)	0.40
PDW polyfit	Gravity direction, ZUPT, torso movement ($\boldsymbol{e}^{(\mathrm{t})} = \boldsymbol{v}^{\mathrm{IMU}} - \boldsymbol{v}^{\mathrm{PDW}}$)	0.42

V. Experiments and Results

A. Experimental Settings

Two IMUs (SS-MS-HMA16G15 by SPORTS SEINSING Inc.) are attached to the left and right insteps, while a LiDAR–IMU unit (VLP-16 by Velodyne Inc. and 3DM-GX5-45 by MicroStrain Inc.) is rigidly mounted on the back (Fig. 1) to measure the surrounding environment. For the experiment, data were collected from a straight walk in a flat indoor corridor with a distance of 20 m. To observe torso movement, we employed LiDAR inertial odometry (LIO) [19], which is more robust and accurate than traditional LiDAR-based odometry, ensuring it can be used as an absolute observation with minimal error.

Table I lists the observations used. The proposed method that fits a polynomial approximation to smooth the point foot velocity data of the PDW model and applies the recalculated velocity from this approximation to the constraint and is referred to as *PDW polyfit*. The methods compared include the approach from [1], which does not account for torso movement (*Without LIO*), and the method from [13], which includes torso movement observations and applies a constraint where foot velocity is considered twice the torso velocity (*LIO velocity ×2*). Additionally, to verify the effect of polynomial approximation on the estimation results, we introduced a method (*PDW normal*), which directly applies the constraints without approximation. To evaluate the impact of the newly added constraints, the comparison for all methods was based on data obtained after individual estimation, with each result not yet integrated.

Using these methods, the weights of the error function related to torso movement observation, denoted as $\boldsymbol{\Omega}_i^{(\mathrm{t})}$, were varied in 10-fold increments from 10^{-8} to 10^{-5}. This was done to assess the impact of the newly added constraints on both estimation accuracy and gait trajectory geometry. The estimation results were qualitatively evaluated based on terminal error and the geometry of trajectory and velocity data in the sagittal plane, focusing on a 3-s period near the end of the walk. Terminal error e refers to the square root of the squared error between the average of the final positions of both feet at the end of the walk and the ground truth $\boldsymbol{x}^{\mathrm{GT}}$.

$$e = \sqrt{\left(\boldsymbol{x}_n^{\mathrm{Left}} + \boldsymbol{x}_n^{\mathrm{Right}}\right)/2 - \boldsymbol{x}^{\mathrm{GT}}}, \boldsymbol{x}^{\mathrm{GT}} = (0, 20, 0) \quad (21)$$

B. Estimation Results and Discussion

Table I presents the terminal error for each method. The weights for the error functions based on torso movement observations to compare differences between methods were determined empirically: 10^{-7} for *LIO velocity ×2* and 10^{-5} for both *PDW normal* and *PDW polyfit*. Adding the observation of torso movement (*PDW normal* and *PDW polyfit*) improved terminal error accuracy by reducing it by more than 17% compared to *LIO velocity × 2*. The larger terminal error observed for *PDW polyfit* compared to *PDW normal* is likely attributed to additional fitting errors introduced by the polynomial approximation process. However, the impact of this additional error is relatively small, approximately 0.02m.

Fig. 6 shows an enlarged view of the 3-s period just before the end of the walk, during which the constraint weights were varied. As the weights increased, the terminal error for *LIO velocity ×2* increased, leading to a distortion of the trajectory shape. In contrast, *PDW normal* preserved the trajectory shape while reducing the terminal error. *PDW polyfit* demonstrated similar performance to *PDW normal*, indicating that the polynomial approximation did not adversely affect the results. This is due to the fact that the error was corrected based on the gait trajectory of the PDW, which allowed the correspondence to be properly considered compared to the *LIO velocity ×2*, improving the accuracy of the constraints and allowing the trajectory shape to be maintained. In addition, the high accuracy of the LIO is reflected in the PDW constraints, leading to an improvement in the terminal error while maintaining the trajectory shape.

Fig. 7 shows a graph comparing the speeds obtained by integrating the raw data 3-s period just before the end of the gait using ZUPT with the modified speeds (*PDW normal* and *PDW polyfit*: 10^{-5}, *LIO velocity ×2*: 10^{-7}) when the terminal error of the trajectory is minimized by each method. The polynomial approximation effectively smooths the drop after the peak. However, it is important to note that the PDW-based constraint assumes that the passive walking trajectory is approximately consistent with the real human walking trajectory. In reality, the PDW trajectory and the real human walking are not completely identical, so it is difficult to claim that the raw data and the corrected speed distributions are equivalent, as shown in Fig. 7. If the constraint weight is increased too much and the constraint becomes too strong, the influence of the PDW information may be too strong and obscure the original walking data. To avoid losing the details of the original movement, both the PDW equation of motion and the fitting method need to be refined to address the inconsistency between the PDW and the real human walking.

VI. Conclusions

In this study, we introduced a method to consider the correspondence between LIO data representing torso movement and IMU data representing foot movement, using a PDW model and applying it to the framework of the gait trajectory estimation method of the previous study. Experiments using real data confirmed that this constraint method enables the gait trajectory geometry to be preserved. However, it is important to recognize that incorporating this

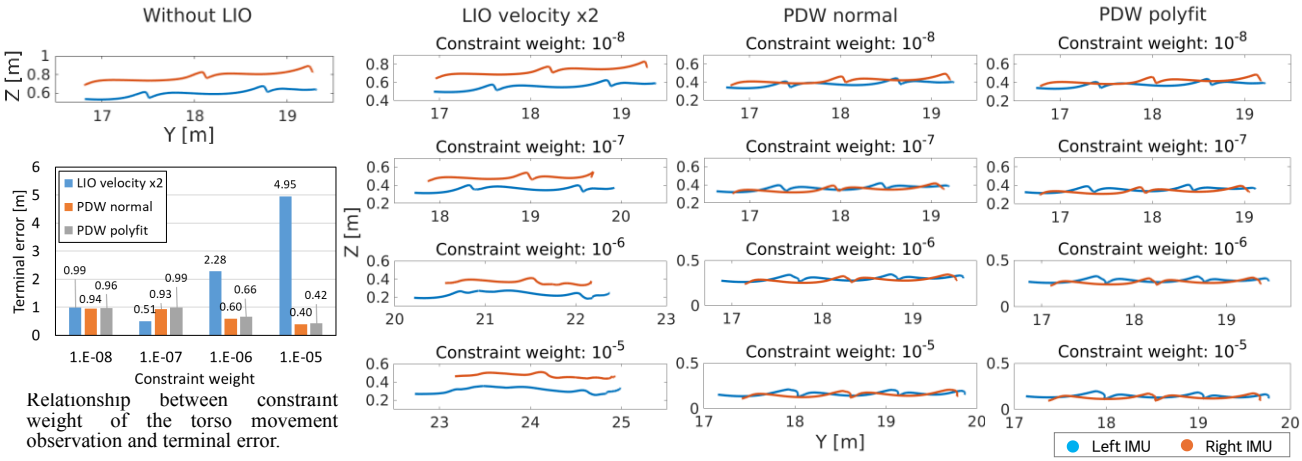

Relationship between constraint weight of the torso movement observation and terminal error.

Fig. 6. Gait trajectory shape in the sagittal plane during 3-s immediately before the end of walking

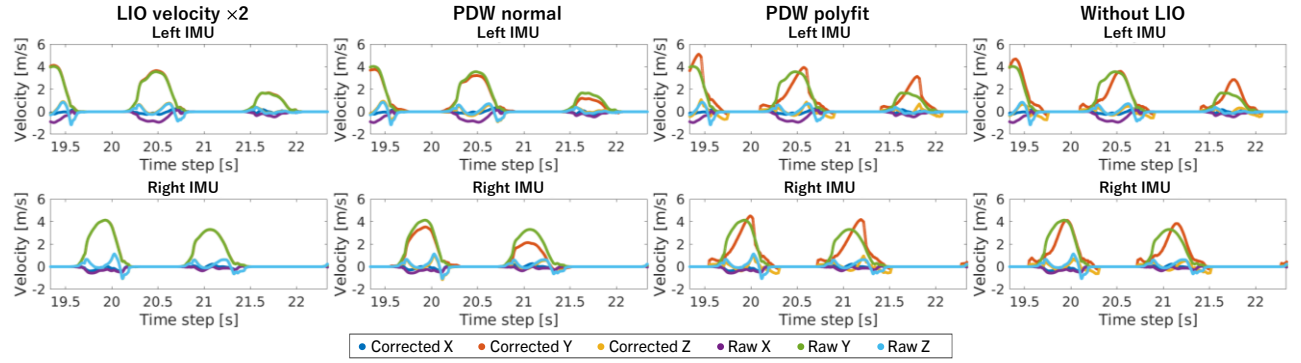

Fig. 7. Raw and corrected velocities in the sagittal plane during 3-s immediately before the end of walking. (Upper panels: left IMU; Lower panels: right IMU. Horizontal axis: time [s]; Vertical axis: speed [m/s])

constraint scan impair the original kinematic information about gait. Further research is needed to determine how to improve the trajectory geometry after integrating information from both feet. This remains a focus for our future work.

REFERENCES

[1] K. Irie, H. Kasai and K. Yamazaki. "An optimization approach to walking motion estimation from dual foot-mounted IMUs," In 28th Robotics Symposia, pp.68–70, 2023.

[2] J. Wahlström, I. Skog, F. Gustafsson, A. Markham, and N. Trigoni. "Zero-Velocity Detection—A Bayesian approach to adaptive thresholding," IEEE Sensors Letters, Vol. 3, No. 6, pp. 1–4, 2019.

[3] E. Foxlin. "Pedestrian tracking with shoe-mounted inertial sensors," IEEE Computer Graphics and Applications, Vol. 25, No. 6, pp. 38–46, 2005.

[4] C. Fischer, P. Talkad Sukumar, and M. Hazas. "Tutorial: implementing a pedestrian tracker using inertial sensors", IEEE Pervasive Computing, Vol. 12, No. 2, pp. 17–27, 2013.

[5] I. Skog et al. "Fusing the information from two navigation systems using an upper bound on their maximum spatial separation," In International Conference on Indoor Positioning and Indoor Navigation (IPIN), pp. 1–5, November 2012.

[6] G. V. Prateek, R. Girisha, K. V. S. Hari, and P. Händel. "Data fusion of dual foot-mounted INS to reduce the systematic heading drift," In 4th International Conference on Intelligent Systems, Modelling and Simulation, pp. 208–213, 2013.

[7] D. D. Pham, Y. S. Suh. "Pedestrian navigation using foot-mounted inertial sensor and LIDAR," Sensors, vol.16, no.1, pp.120–136, 2016.

[8] Y. Wang, S. Askari, C.-S. Jao, and A. M. Shkel, "Directional Ranging for Enhanced Performance of Aided Pedestrian Inertial Navigation," presented at the IEEE International Symposium on Inertial Sensors and Systems, 2019.

[9] A. Ahmed and S. Roumeliotis, "A visual-inertial approach to human gait estimation," 2018 IEEE International Conference on Robotics and Automation (ICRA), Brisbane, QLD, Australia, pp.4614-4621, 2018.

[10] Yudi Dai, Yitai Lin, Chenglu Wen, Siqi Shen, Lan Xu, Jingyi Yu, Yuexin Ma, and Cheng Wang. "HSC4D: Human-centered 4D scene capture in large-scale indoor-outdoor space using wearable IMUs and LiDAR," In Proceedings of the IEEE/CVF Conference on Computer Vision and Pattern Recognition (CVPR), pages 6792–6802, June 2022.

[11] Vladimir Guzov, Aymen Mir, Torsten Sattler, and Gerard Pons-Moll. "Human POSEitioning System (HPS): 3D human pose estimation and self-localization in large scenes from body-mounted sensors," In Proceedings of the IEEE/CVF Conference on Computer Vision and Pattern Recognition,pages 4318–4329, 2021.

[12] K. Irie. "A graph optimization approach for motion estimation using inertial measurement unit data," ROBOMECH Journal, Vol. 5, No. 1, p. 14, 2018.

[13] H. Kasai, K. Irie and K. Yamazaki. "Combining LiDAR odometry with walking motion estimation using bilateral instep-mounted IMUs," The 24th Annual Conference of System Integration (SI2023), 1H6-14, 2023.12.14. (In Japanese)

[14] T. McGeer. "Passive Dynamic Walking," The International Journal of Robotics Research, vol.9, no.2, pp.62–82, 1990.

[15] T. McGeer. "Passive walking with knees," Proceedings., IEEE Int'l Conf. on Robotics and Automation, pp.1640–1645, 1990.

[16] Zang X, Liu X, Zhu Y, Zhao J. "Study of human walking patterns based on the parameter optimization of a passive dynamic walking robot," Technol Health Care. 2016 Apr 29;23-suppl 2:S849-58.

[17] Chen, Hsu. "Passive dynamic walking with knees: A point foot model," PhD Thesis. Massachusetts Institute of Technology, 2007.

[18] J. Diebel. "Representing attitude: Euler angles, unit quaternions, and rotation vectors," Technical Report, Stanford University, 2006.

[19] W. Xu, Y. Cai, D. He, J. Lin and F. Zhang, "FAST-LIO2: Fast Direct LiDAR-Inertial Odometry," in IEEE Transactions on Robotics, vol. 38, no. 4, pp. 2053-2073, Aug. 2022.